

**Vertical Axis Wind Turbine with  
Continuous Blade Angle Adjustment**

by

Samuel Bruce Weiss

Submitted to the Department of Mechanical Engineering  
in Partial Fulfillment of the Requirements for the Degree of

Bachelor of Science

at the

Massachusetts Institute of Technology

June 2010

©2010 Massachusetts Institute of Technology  
All rights reserved

Signature of Author .....

Department of Mechanical Engineering  
May 7, 1993

Certified by .....

Sanjay E. Sarma  
Associate Professor of Mechanical Engineering  
Thesis Supervisor

Accepted by .....

John H. Lienhard V  
Collins Professor of Mechanical Engineering  
Chairman, Undergraduate Thesis Committee

# Vertical Axis Wind Turbine with Continuous Blade Angle Adjustment

by

Samuel Bruce Weiss

Submitted to the Department of Mechanical Engineering  
on May 10, 2010 in partial fulfillment of the  
Requirements for the Degree of Bachelor of Science in  
Mechanical Engineering

## ABSTRACT

The author presents a concept for a vertical axis wind turbine that utilizes each blade's entire rotational cycle for power generation. Each blade has its own vertical axis of rotation and is constrained to rotate at the rate of one half of a revolution per full revolution of the rotor. For a rotor of radius  $r$  and blades of width  $b$ , a technical analysis predicts a theoretical maximum power coefficient of  $C_P = \frac{b}{2r+b}$ , neglecting wind flow interference by upwind blades. This theoretical power coefficient is generally greater than the efficiency of a typical Savonius wind turbine ( $C_P \approx 0.15$ ), and it reaches  $C_P = 0.5$  at the limiting blade width,  $b = 2r$ . The analysis also predicts a static torque and optimal tip-speed ratio that are both greater than those of a Savonius wind turbine with similar blade dimensions.

Design considerations for implementing the kinematic constraint and for blade adjustment to account for changes in wind direction are discussed, and the author's prototype is presented. Testing of the prototype demonstrated that implementation of the kinematic constraint is feasible, and that efficiencies greater than those achievable by a Savonius turbine are plausible. In  $4 \frac{\text{m}}{\text{s}}$  wind conditions, the prototype yielded an estimated  $C_P$  of 0.15, with much room for improvement through design changes and blade optimization in future iterations of this style of turbine.

Thesis Supervisor: Sanjay E. Sarma

Title: Associate Professor of Mechanical Engineering.

## **Acknowledgements**

The author is grateful for the supervision, guidance, and support of Sanjay Sarma throughout the development of this thesis project. He would also like to thank Bill Buckley, David Dow, and Patrick McAtamney for their help in the construction of the turbine prototype.

# Contents

<b>1</b>	<b>Introduction</b>	<b>6</b>
1.1	Types of Wind Turbines . . . . .	6
1.2	The Savonius Wind Turbine . . . . .	7
<b>2</b>	<b>Literature Review</b>	<b>8</b>
2.1	Swinging Blade Design . . . . .	8
2.2	Pitch Angle Adjusting Turbines . . . . .	9
2.3	Similar Concepts . . . . .	9
<b>3</b>	<b>Concept</b>	<b>10</b>
3.1	Blade Movement . . . . .	10
3.2	Blade Angle Control . . . . .	12
3.3	Advantages . . . . .	12
3.4	Disadvantages . . . . .	13
<b>4</b>	<b>Theoretical Analysis</b>	<b>14</b>
4.1	Lift and Drag Forces . . . . .	14
4.2	Static Torque . . . . .	15
4.3	Dynamic Analysis . . . . .	16
4.4	Flow Interference . . . . .	19
<b>5</b>	<b>Design and Prototype</b>	<b>20</b>
5.1	Machine Design . . . . .	21
5.2	Kinematic Constraint Implementation . . . . .	21
5.3	Blade Angle Control . . . . .	21
5.4	Blade Design . . . . .	23
5.5	Testing . . . . .	24
<b>6</b>	<b>Conclusions</b>	<b>25</b>
6.1	Optimization . . . . .	25
	<b>References</b>	<b>26</b>

## List of Figures

1	Savonius Turbine . . . . .	7
2	Swinging Blade Design . . . . .	9
3	Blade movement for turbine with continuous blade rotation . . . . .	11
4	Lift and drag forces acting on turbine blade . . . . .	15
5	Blade movement in dynamic case . . . . .	16
6	Torque on turbine blades during rotation . . . . .	17
7	Torque on blade for different rotor-tip speed ratios, and Power-Speed curve .	18
8	Two-dimensional flow analysis in static case . . . . .	20
9	Solid model views of turbine prototype . . . . .	22
10	Turbine prototype and qualitative testing . . . . .	24

# 1 Introduction

Wind turbines and windmills have been in use for centuries for a variety of applications, and there is a constant effort to modify and improve their design. This paper presents a concept, analysis, and design of the authors idea for a drag-based vertical axis wind turbine that utilizes each blade's entire rotational cycle for power generation. This paper supplements a mechanical prototype intended to demonstrate the kinematic constraints and mechanical mechanisms required by this design.

## 1.1 Types of Wind Turbines

Most wind turbines can be classified according to two main attributes. The first is the method of power generation; turbines are called lift-based or drag-based depending on their primary source of propulsion. The second is the orientation of the axis of rotation of the turbine, which can be horizontal (almost always parallel rather than transverse to the wind flow) or vertical (transverse to the wind flow). Each combination of axis orientation and power generation method has its own advantages and disadvantages, which are briefly discussed here.

Lift-based wind turbines (especially horizontal turbines) are the most common turbine used for large-scale power generation. They tend to have much-higher rotational speeds, which reduces power loss when connecting a turbine to a generator. The relatively small surface area of their narrow blades also gives lift-based turbines a fairly high power-to-weight ratio. Drawbacks of lift-based turbines include the requirement of precise blade shaping and balancing, as well as (in the case of horizontal turbines) inefficiencies at small scale. Drag-based turbines, on the other hand, are often preferred for applications that require direct application of mechanical work (e.g. milling corn, for a windmill) because of the high rotor torque, or for fulfilling small-scale power requirements. [7]

Horizontal axis turbines are often easier and more efficient to scale (by extending a tall, vertical tower) than their vertical counterparts. Horizontal axis turbines also experience little variable interference of the wind flow between blades, whereas with a vertical axis turbine there is direct and unavoidable interference. Vertical turbines, however, are often more easy to install and repair since their machinery for power generation is usually located

at ground level, whereas horizontal axis turbines’ machinery is high off the ground at the rotor’s center. [7]

Examples of these types of turbines include modern power-generating wind turbines (horizontal, lift-based), 12th century European windmills (horizontal, drag-based), Darrieus wind turbines (vertical, lift-based), and Savonius turbines (vertical, drag-based). A wealth of information is available for each of these types of turbines, but we will focus on discussing some details of the vertical, drag-based, Savonius turbine as it relates most closely to the wind turbine concept presented in this paper.

## 1.2 The Savonius Wind Turbine

Perhaps the most prevalent vertical axis wind turbine is the S-shaped, Savonius wind turbine. The Savonius turbine consists of cupped blades that catch the wind to generate power (see Fig. 1). Power generation is possible because of blade geometry — the cupped blades have a higher drag coefficient when moving with the wind than when moving against the wind. The difference between the torque on the blades traveling downwind and the blades traveling upwind gives the net torque about the generator.

There are several important parameters that we will use to characterize the ability of the Savonius turbine to generate power (these will also be used to compare the new design to the Savonius turbine). The first is *tip speed ratio*,  $\lambda$ , which is defined as the ratio between a blade’s speed at its tip and the faraway wind velocity. For a turbine of radius  $R$ , spinning at angular rate  $\omega$ , in a wind with faraway velocity  $v_0$ , we have

$$\lambda = \frac{R\omega}{v_0}. \tag{1}$$

We can also define a turbine’s efficiency, also known as its *power coefficient*,  $C_P$ , as the ratio between the power produced by the turbine and the power contained in the wind that passes through the reaches of the turbine blades. If we define the swept area,  $A_S$  as the

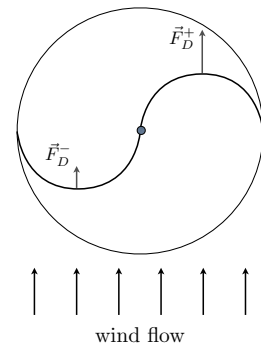


**Figure 1:** An S-shaped, Savonius turbine. Positively contributing drag forces ( $F_D^+$ ) outweigh negatively contributing drag forces ( $F_D^-$ ) to create a net positive torque about the rotor center.

cross-sectional area of the wind flow that the turbine blades pass through, then a turbine that produces power  $P$  has efficiency

$$C_P = \frac{P}{\frac{1}{2}\rho A_S v_0^3}, \quad (2)$$

where  $\rho$  is the air density. A typical Savonius turbine achieves an efficiency of  $C_P = 0.12$  to  $0.15$  at a tip speed ratio of about  $\lambda = 0.7$ , [6, 9] but an optimized Savonius turbine, studied both theoretically and empirically by Modi and Fernando, can reach a peak efficiency of  $C_P = 0.32$  at a tip speed ratio of  $\lambda = 0.8$ . [6]

A turbine’s start-up wind velocity and static torque can also be important parameters. The start-up wind speed is the lowest wind speed at which the turbine spins (if it is self-starting, at all). This is typically on the order of a few meters per second, but depends heavily on turbine design and construction. The static torque is the torque that the wind applies about the rotor center when the rotor is fixed. The static torque is often a function of rotor angle, and a high static torque often indicates a low start-up wind speed.

## 2 Literature Review

Many other variations of drag-based vertical axis turbines have been designed, prototyped, and implemented for power generation. Documented in this section is prior research on the two types of turbines that provided the main inspiration behind the author’s own design. Other vertical axis turbines that are similar in concept to the author’s design are also discussed.

### 2.1 Swinging Blade Design

Several turbine designs have sought to eliminate the negative drag that acts on the blades traveling upwind in a Savonius turbine. Many of these employ slatted, or “swinging” blades that are constrained to trap wind during their downwind travel, but swing freely (and thereby reduce or eliminate drag) during their upwind travel (see Fig. 2).



Tabassum and Probert investigated a slatted design and found that the design increased startup torque by as much as 35 percent over a standard Savonius wind turbine, and confirmed that the net static torque on the rotor was positive for every rotor orientation. [10]

Further investigation into the slatted design by Reupke and Probert confirmed that this style turbine was self-starting, and that it had a slightly higher optimal tip speed ratio (approximately 0.8) than a typical Savonius turbine (approximately 0.7). This slatted design yielded a slightly greater torque than a Savonius turbine at low speeds, but the centrifugal forces of the swinging blades severely hurt the turbine’s efficiency at high speeds. As a result, it’s peak power coefficient only reached 0.05, compared to 0.18 for a similarly constructed Savonius turbine. [8]

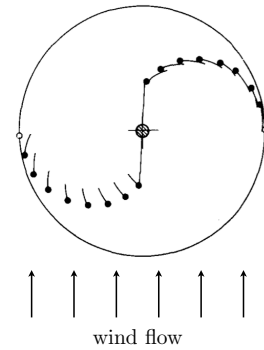


**Figure 2:** A modified depiction of Reupke and Probert’s slatted blade design. Blade segments are free to swing to reduce drag during upwind travel. [8]

## 2.2 Pitch Angle Adjusting Turbines

Hwang et. al. discuss a modification of a lift-based vertical turbine that varies the pitch of its blades slightly as the turbine rotates. By optimizing the pitch angle based on the blade’s position, the lift force is increased, and power generation increased by 30 percent over a turbine with fixed pitch angles. [4]

## 2.3 Similar Concepts

The author has found that other individuals have attempted their own implementations of a concept similar to his own. Unfortunately, the author did not identify these similar vertical axis wind turbines until very late in the course of his research, largely due to their foreign origin. Descriptions based on the author’s understanding of the projects is included for completeness, and it is likely that the author’s own design could be improved upon through feedback from these other attempts.

A similar turbine created by French inventor Pierre Dieudonne consists of two levels of blades with a similar kinematic constraint, but with the two levels rotating in opposite directions. His website and videos are in French, and so the author’s understanding is almost entirely from the images that Dieudonne provides. [2]

The author has also found limited information on a turbine recently produced by a Chinese company, Jiangsu Wynch Corp., Ltd., that appears to employ a similar kinematic constraint. This turbine is supported by a tall stand to reach a higher altitude, and has much narrower blades than the author’s prototype. [5]

### 3 Concept

The purpose of the author’s drag-based vertical axis turbine design is to utilize the entire rotational cycle of each blade for positive power contribution. Typical Savonius wind turbine blades detract from the net torque on the rotor as they rotate into the wind; net positive power generation is possible only because the drag coefficient of the blades in their downwind orientation exceeds that of the blades in their upwind orientation. While other designs, such as those that employ blade flaps, seek to essentially eliminate all forces on the turbine blades during their upwind travel, the author’s design is more ambitious in that it seeks to utilize this regime for positive power generation. The potential applications of this new design are expected to be similar to that of Savonius turbines — small scale power and direct mechanical work — but with several advantages as discussed in Section 3.3.

#### 3.1 Blade Movement

To create positively contributing torque on each blade at every point throughout the turbine’s rotation, the angle of each blade is continuously adjusted to attain a near-optimal combination of drag and lift. The blade passes through four main phases as the turbine rotates (see Fig. 3):

1. Blade moving parallel to wind — the blade face is roughly perpendicular to the wind flow, and drag forces on the blade dominate.

2. Blade moving perpendicular to wind, behind turbine axis — here, the blade is oriented so that both lift and drag forces contribute positively to power generation.
3. Blade moving into wind — in this regime the blade is oriented to minimize drag, and lift forces dominate and contribute positively to power generation.
4. Blade moving perpendicular to wind, in front of turbine axis — as in Phase 2, both lift and drag forces act on the blade and contribute positively to power generation.

In the course of this movement, each turbine blade performs one half-rotation per full revolution of the turbine. The key to this turbine design is this kinematic constraint: relative to the inertial reference frame, each blade is constrained to rotate at a 1:2 ratio with respect to the rotor.

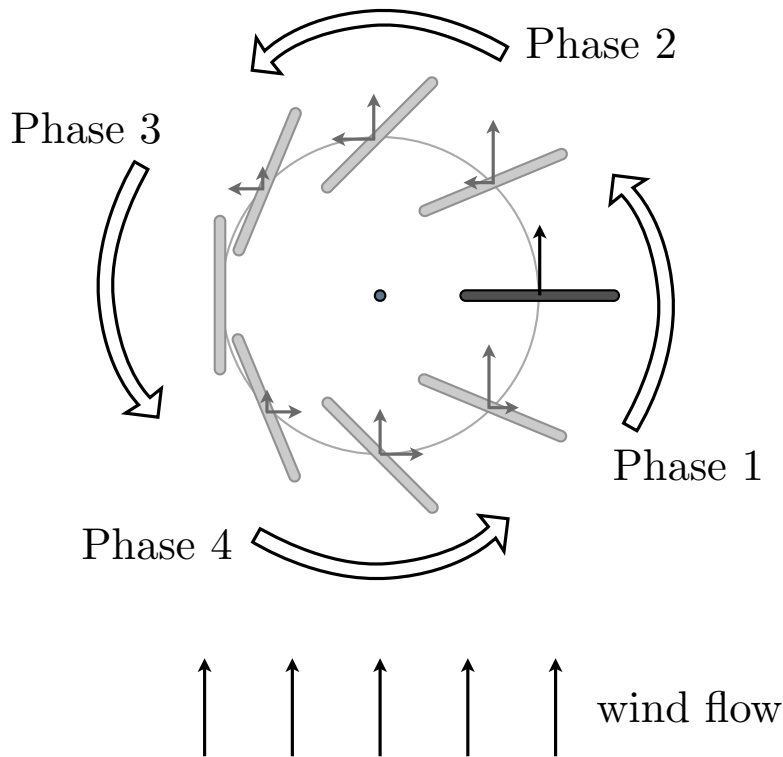


**Figure 3:** Depiction of several blade orientations as the turbine rotates. Drag forces (vertical force vectors) on the blades contribute more heavily when the blade is moving with the wind, and lift forces (horizontal force vectors) dominate when the blade is moving into the wind. The orientation of the blade at each point results in a positively contributing torque on the rotor. (Note that small frictional drag forces are neglected.)

The implementation of this kinematic constraint is discussed in Section 5, and an analysis of the drag and lift forces on the turbine blades is presented in Section 4.

## 3.2 Blade Angle Control

Because of the 1:2 ratio of blade to turbine rotation, the blade orientation is not independent of wind direction. An integrated mechanism is required to either actively or passively orient the blades, or the entire turbine, to account for a shift in wind direction. The design of the prototype turbine incorporates a mechanical system that adjusts all blade angles simultaneously so that each blade continues to square up as it is moving parallel to the wind flow (see Section 5.3). Such a mechanical system could be either passively controlled (by a weather vane, for instance) or actively controlled (by a sensor and actuator).

## 3.3 Advantages

The primary advantage of this design over most drag-based vertical axis wind turbines, like the Savonius turbine and its variants, is that, through the harvesting of both lift and drag forces, power is generated by every blade throughout the turbine's entire rotation. This design, therefore, is expected to be more efficient than a standard Savonius turbine or its variants, as discussed in Section 4.3.

This type of turbine also decreases the horizontal reaction force required to support the turbine when compared to a Savonius turbine. For a vertical axis wind turbine, the supporting force is approximately equal to the sum of the lift and drag force vectors on the blades. Since a Savonius turbine incurs both positive and negatively contributing drag forces on its blades, a portion of these forces cancel each other out with respect to power generation, but combine to increase the required reaction force. The new design, however, eliminates negative drag forces, and thus reduces the required reaction force to support a turbine generating the same amount of power.

There are several other advantages that this turbine design could have over typical vertical axis wind turbines. While some vertical turbines are either not self-starting, or can only self-start from certain rotational positions, a turbine of this design will be able to start from

any position since every blade is always contributing positive torque. For the same reason, this style of turbine is expected to have a higher static torque than a Savonius turbine (see Section 4.2).

One drawback of most drag-based turbines is a low tip-speed. While this design does not solve that issue by any means, this turbine's theoretical optimal tip speed is slightly greater than that of a Savonius turbine with similarly-dimensioned blades because, in this new design, blades traveling into the wind are also generating power.

### 3.4 Disadvantages

As with most design alternatives, this vertical axis turbine design has drawbacks that need to be weighed against its advantages. The most severe drawback is the added complexity of the new design. The kinematic constraint requires more moving parts — the blades are no longer fixed rigidly to the rotor — and this change eliminates much of the simplicity of a Savonius turbine. This complexity will likely add to construction and maintenance costs, and this tradeoff needs to be weighed against any gain in power-generation.

The kinematic constraint also requires a specific blade orientation at each rotational position, meaning that, unlike a Savonius turbine, an adjustment needs to be made to account for a change in wind direction. As previously mentioned, this is a solvable problem, but it is another issue that increases the complexity of this style of turbine.

A danger of the added complexity is that it could actually hurt the overall performance of this turbine relative to other vertical axis wind turbines. Additional moving parts create additional friction surfaces that detract from power generation. The added weight from the mechanical systems used to orient the blade could also decrease turbine efficiency.

Furthermore, since each blade rotates only one half of a revolution per full revolution of the rotor, there is less freedom in blade design and optimization than with other vertical axis wind turbines. Each blade must be  $180^\circ$  rotationally symmetric so that there is no difference in drag or lift forces between consecutive rotations. If blades are rigid, then they likely cannot be scooped as in an S-shaped Savonius turbine. This issue and alternative blade designs are discussed further in Section 5.4.

And finally, this turbine is still a drag-based vertical axis turbine. While it may generate more power than a Savonius turbine, it is still limited in its tip speed and power generation when compared to lift-based, horizontal turbines. As with a Savonius turbine or any variant, it's applications are likely restricted to small-scale electric power generation or the direct production of mechanical power.

## 4 Theoretical Analysis

The analysis performed in this section will assume thin, flat, and rigid turbine blades. Each blade is assumed to pivot about a point that is a distance  $r$  from the center of the rotor, and is kinematically constrained as discussed in Section 3.1 — each blade performs one half of a rotation per full revolution of the rotor. For a given rotational position of the rotor,  $\theta$ , the flat blade makes an angle  $\alpha$  with respect to its initial position (or more specifically, with respect to a vector perpendicular to the wind flow vector,  $\vec{v}_0$ ). Because of the kinematic constraint imposed on the blades, we necessarily have  $\alpha = \frac{\theta}{2}$ . The majority of our analysis will consider the blade that begins perpendicular to the wind when the rotor is at position  $\theta = 0$  (see Fig. 4).

### 4.1 Lift and Drag Forces

Each blade has acting on it a lift force and a drag force,  $\vec{F}_L$  and  $\vec{F}_D$ , respectively, which sum to a net force  $\vec{F}_{net} = \vec{F}_L + \vec{F}_D$  (for this analysis we will neglect the smaller frictional drag forces on the blades). We can define lift and drag coefficients,  $C_L$  and  $C_D$ , as

$$C_L = \frac{F_L}{\frac{1}{2}\rho v_0^2 A} \quad \text{and} \quad C_D = \frac{F_D}{\frac{1}{2}\rho v_0^2 A}, \quad (3)$$

where  $\rho$  is the air density,  $v_0$  the faraway fluid velocity, and  $A$  the area of the blade face. There exist numerous complex approximating curves for these drag and lift coefficients. For this analysis, we will use a fairly simple approximation for the lift and drag coefficients on a flat plate presented by Caplan and Gardner [1] due to its ease of manipulation. It is reasonably close enough to approximations presented by Hoerner and others for this analysis. [3]

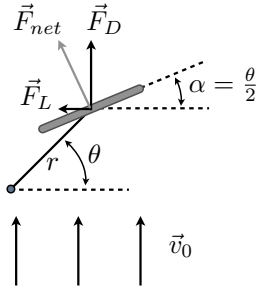


**Figure 4:** Lift and drag forces acting on a blade yield a net force approximately normal to the blade face. The blade angle,  $\alpha$  is constrained to be half the rotor angle  $\theta$ .

Caplan and Gardner find that, for a flat plate,

$$C_L = C_{L\max} \sin(2\alpha) \quad \text{and} \quad C_D = 2C_{L\max} \cos^2(\alpha), \quad (4)$$

with  $C_{L\max}$  in the approximate range of 1.0 to 1.2 (we will use  $C_{L\max} = 1$  in any calculations). These approximations, and hence the majority of this analysis, ignore any flow-path interference between blades. Section 4.4 briefly discusses this assumption, but an actual dynamic flow path analysis is outside of the scope of this report. Note that with these approximations for the lift and drag coefficients, we have

$$\frac{F_L}{F_D} = \frac{C_L}{C_D} = \frac{C_{L\max} \sin(2\alpha)}{2C_{L\max} \cos^2(\alpha)} = \tan \alpha. \quad (5)$$

This result (typically expressed as  $\frac{F_D}{F_L} = \tan(\frac{\pi}{2} - \alpha)$  for our definition of  $\alpha$ ) implies that the net force on the blade,  $\vec{F}_{net}$ , is approximately normal to the blade face.

## 4.2 Static Torque

When the turbine is stationary, each blade provides a net torque on the rotor equal to

$$\Gamma = F_L r \sin \theta + F_D r \cos \theta. \quad (6)$$

Substituting in the expressions for the lift and drag forces from Equation (3), as well as for the lift and drag coefficients of Equation (4) gives

$$\Gamma = \frac{1}{2} \rho v_0^2 A r C_{L\max} (\sin(2\alpha) \sin(\theta) + 2 \cos^2 \alpha \cos \theta). \quad (7)$$

Substituting  $\alpha = \frac{\theta}{2}$  into Equation (7) and simplifying gives

$$\Gamma = \frac{1}{2} \rho v_0^2 A r C_{L\max} (1 + \cos \theta), \quad (8)$$

which is an elegant approximation for the static torque generated by each blade at rotor position  $\theta$ . Noting that  $\sum_{j=0}^{n-1} 1 + \cos(\theta + \frac{2\pi j}{n}) = n$  for all  $\theta$ , for  $n \geq 2$ , it follows that the approximate net torque on the rotor from any number of evenly-spaced blades,  $N \geq 2$ , is

$$\Gamma = N \cdot \frac{1}{2} \rho v_0^2 A r C_{L \max}. \quad (9)$$

Without flow interference from the upwind blades, static torque would increase linearly with the number of blades, as well as with blade area and rotor radius, and would be independent of rotor orientation (implying that the turbine should indeed be self-starting from any rotor orientation).

### 4.3 Dynamic Analysis

When the turbine is in motion, we must take into account the effects of the rotor movement on the lift and drag coefficients, as well as on the relative wind speed for each blade. Assuming that the turbine is spinning an angular rate of  $\dot{\theta} = \omega$ , the center of each blade is traveling at a speed  $v_b = r\omega$  (see Fig 5). The velocity vector of the blade center is  $\vec{v}_b = -v_b \sin \theta \hat{x} + v_b \cos \theta \hat{y}$ , and the relative wind velocity at the blade center,  $\vec{v}_r$ , is

$$\vec{v}_r = \vec{v}_0 - \vec{v}_b = v_b \sin \theta \hat{x} + (v_0 - v_b \cos \theta) \hat{y}. \quad (10)$$

We will assume that this is the relative wind speed across the whole blade — i.e. we will neglect the fact that the blade is also rotating at a rate of  $\frac{\omega}{2}$  with respect to an inertial reference frame. Although an imperfect assumption, it is a more accurate than it would be in the case of a typical Savonius turbine, where each blade is rotating at a rate of  $\omega$  with respect to an inertial reference frame.

This relative wind velocity gives both a new effective wind speed and a new effective wind direction (and thus a new effective  $\alpha$  for calculating the lift and drag coefficients in Equation 4). These are:

$$v_{eff} = |\vec{v}_r| \quad (11)$$

and

$$\alpha_{eff} = \frac{\theta}{2} - (\angle \vec{v}_r - \angle \vec{v}_0), \quad (12)$$

where we know  $\angle \vec{v}_0 = \frac{\pi}{2}$ .

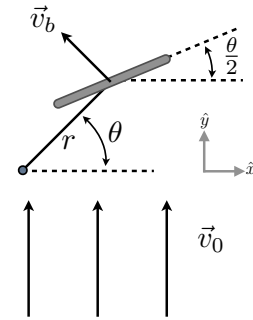


**Figure 5:** Blade movement and coordinate system for dynamic analysis. The wind velocity relative to the blade is  $\vec{v}_r = \vec{v}_0 - \vec{v}_b$ .



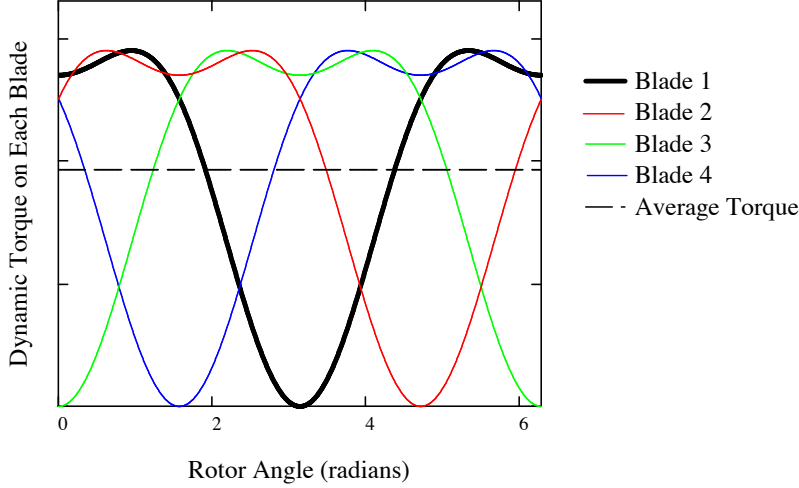


**Figure 6:** Torque on each of four blades during rotation, neglecting flow interference, with a rotor-tip speed ratio of  $k = 0.3$ . The first blade, which is perpendicular to the wind flow when  $\theta = 0$ , is highlighted for clarity.

At this point a symbolic analysis ceases to provide much insight, but plots generated by a numerical analysis demonstrate the trends that we might expect. The torque on each of four blades as a function of the rotor angle,  $\theta$ , is plotted in Fig. 6 for a rotor-tip speed ratio of  $k = 0.3$  (explained in the next paragraph).

For this style of turbine, we can define a *rotor-tip speed ratio*,  $k$ , as

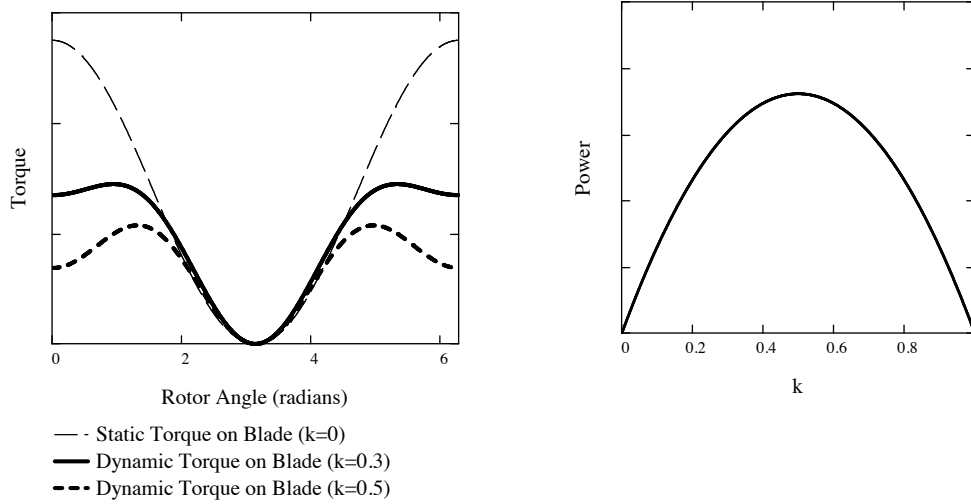
$$k = \frac{v_b}{v_0} = \frac{r\omega}{v_0}. \quad (13)$$

The rotor-tip speed ratio differs from the more traditional tip speed ratio,  $\lambda$  (defined in Equation 1), in that the radius used is based on the blade's center, and not on the blade's tip. The rotor-tip speed ratio can be related to the tip speed ratio by determining what the tip speed of the rotor would be if it were extended to the tip of the blade at position  $\theta = 0$ . For a blade width  $b$  and rotor radius  $r$ , we have

$$\lambda = k \cdot \left(1 + \frac{b}{2r}\right) = k \cdot c \quad (14)$$

where the constant  $c$  can range from 1 to 2, depending on the blade width. An intermediate value of  $c = 1.5$  (when  $b = r$ ) is assumed for the torque and power calculations graphed later. While  $\lambda$  is a more useful quantity for comparing this turbine's tip speed ratio with that of other turbines,  $k$  better allows us to plot torque and power curves not dependent on blade width (when neglecting flow interference).

The static torque on each blade (i.e. the torque when  $k = 0$ ) as well as dynamic torque on each blade (for  $k = 0.3$  and  $0.5$ ) are plotted as functions of rotor angle,  $\theta$ , in Figure 7a. Figure 7b shows turbine power as a function of rotor-tip speed,  $k$ . Given our initial assumptions, we find that the turbine has a peak power output at  $k = 0.5$ , which corresponds to a tip speed of  $\lambda = 0.75$  when  $b = r$  (although this could be as large as  $\lambda = 1.0$  for a turbine with blades just wide enough to just reach the turbine center,  $b = 2r$ ).



(a) Torque vs. Rotor Angle

(b) Power vs. Rotor-Tip Speed Ratio

**Figure 7:** (a) Torque as a function of rotor angle,  $\theta$ , for several rotor-tip speed ratios,  $k$ .  $k = 0$  represents the static torque on the rotor from each blade, and  $k = 0.5$  is the case of optimal power generation. (b) Power vs. rotor-tip speed ratio, with a clear peak at a rotor-tip speed ratio of approximately  $k = 0.5$ . The relationship between  $k$  and tip speed ratio,  $\lambda$ , is given in Equation (14).

Given the assumptions above (e.g. no flow interference, and ignoring blade rotation), we can evaluate the power coefficient,  $C_P$  (defined in Equation 2), at the optimal rotor-tip speed ratio. For a rotor radius  $r$  and a blade width  $b$  and height  $h$ , the swept area is conservatively given as

$$A_S = (2r + b)h. \quad (15)$$

(This value for  $A_S$  assumes that the turbine width is equal to the rotor diameter plus the blade width, even though the blade tip never actually reaches a point  $r + \frac{b}{2}$  away from the turbine's center during upwind travel.) Since the torque on each blade is proportional to its

area,  $A = bh$ , we expect the power coefficient to be proportional to  $\frac{A}{A_S} = \frac{b}{2r+b}$ . Numerically calculating the power produced given the dynamic movement of the blade shows that the missing constant of proportionality happens to be 1.00, so we have

$$C_P = \frac{b}{2r+b} = \frac{\frac{b}{r}}{2 + \frac{b}{r}}. \quad (16)$$

The theoretical power coefficient, therefore, depends only on the ratio of blade width to rotor radius. This ratio ranges from 0 ( $b = 0$ ) to 2 ( $b = 2r$ ), and so  $C_P$  can range from 0 to 0.50, although for values of  $\frac{b}{r}$  close to 2, flow interference will likely have a significant effect, and would reduce  $C_P$  from this theoretical value. For  $b = r$ , the turbine still achieves a theoretical efficiency of 0.33, on par with the most optimized Savonius turbines (see Section 1.2).

#### 4.4 Flow Interference

It is beyond the scope of this analysis to attempt to accurately predict the dynamic interference that the blades effect on the wind flow. It is probably possible to approximate the effect of the interference on the forces on each blade as a function of  $\theta$ ,  $v_0$ , and  $k$ , as well as blade geometry, and then modify the torque and power outputs accordingly. At this point, however, any selection of such a function would be arbitrary and would lend no additional insight.

A rudimentary 2-dimensional flow analysis in the static case at rotor position  $\theta = 0$  was performed for  $v_0 = 4 \frac{\text{m}}{\text{s}}$  and  $b = r = 0.5 \text{ m}$ , and is shown in Fig. 8. The flow paths qualitatively suggest that, while the wind energy is certainly reduced by the time it hits the rear blade, it is not by any means eliminated. Interference effects might be further mitigated when the rotor is spinning, since the relative wind speed,  $|\vec{v}_r|$ , tends to be less than  $v_0$  for the interfering blades.

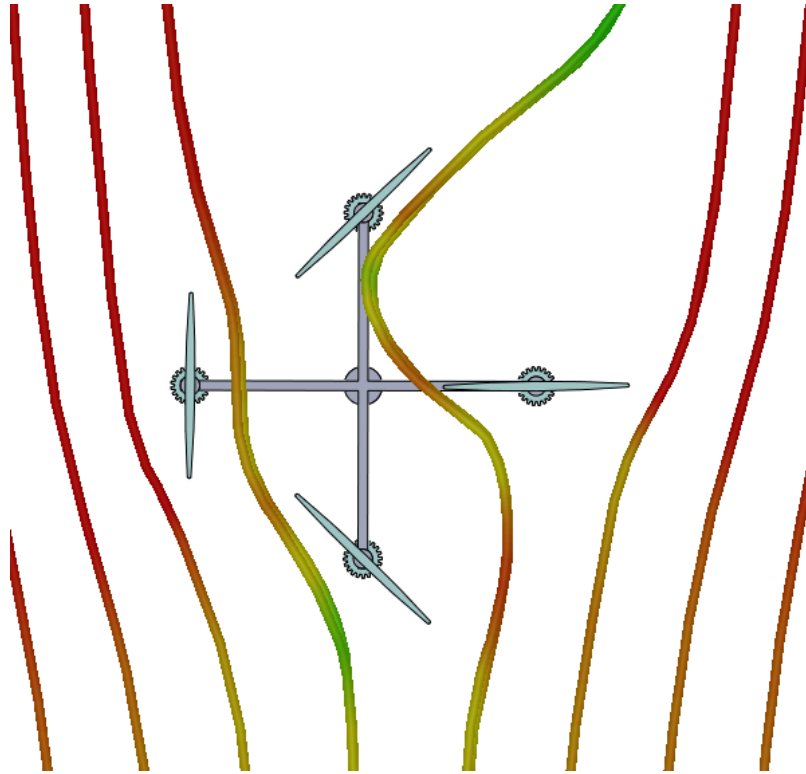


**Figure 8:** Qualitative flow analysis for a static rotor at position  $\theta = 0$ , with a wind speed of  $v_0 = 4 \frac{m}{s}$  and turbine geometry  $b = r = 0.5$  m. Thick lines indicate flow paths, and blank voids indicate blade wakes. While some flow interference does occur, significant drag and lift forces will still be applied to the rear blade.

## 5 Design and Prototype

A large component of this project was the design and construction of a prototype version of this wind turbine. The primary purpose of the prototype was to demonstrate viable implementations of the kinematic constraint on the blade rotation and blade angle adjustment. Future goals include optimizing the turbine design, more precisely measuring its performance, and comparing its performance to that of a Savonius turbine.

This section explains the key design elements of the prototype, discusses challenges relating to any implementation of this turbine concept, and gives results from preliminary testing.

## 5.1 Machine Design

The prototype design (Fig. 9a) consists of three main assemblies (Fig. 9c): a central shaft that is used to constrain blade angles (Section 5.2); a rotor assembly that supports the central shaft through angular contact bearings and also supports the blades; and a base assembly that supports the rotor and that would hold the machinery and electronics required for power generation and blade control (Section 5.3).

The prototype turbine had a rotor radius of  $r = 0.38$  m, a blade width of  $b = 0.30$  m, and a blade height of  $h = 0.48$  m.

## 5.2 Kinematic Constraint Implementation

Elegantly implementing the required kinematic constraint between the blade and rotor rotation was the most difficult task from a design standpoint. The prototype uses a chain-driven system, in which gears on a central shaft (concentric and interior to the rotor) are linked to larger gears on the blade axles (see Fig. 9b). A gear ratio between the central and satellite gears of 1:2 creates the required kinematic constraint. During normal operation, the central shaft is held fixed (relative to the ground). Each rotation of the rotor results in a half rotation of each satellite gear, and thus a half rotation of each blade, as required.

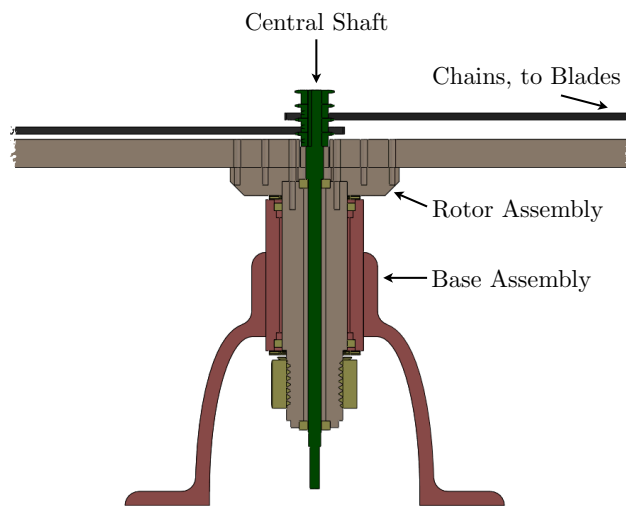
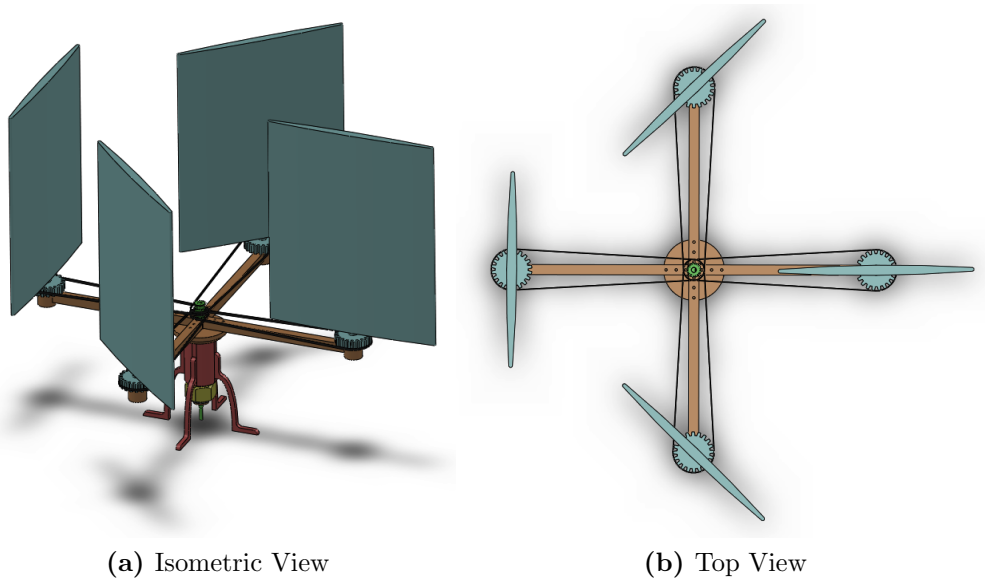
## 5.3 Blade Angle Control

The 1:2 gear ratio between the central gear and satellite gears, described above, greatly simplifies the issue of adjusting the angles of the blades to account for a change in wind direction. In fact, if the wind direction shifts by an angle  $\beta$ , then the central gears need only be rotated by the same angle  $\beta$  and in the same direction as the wind change. Due to the wind shift, the new rotor angle is

$$\theta' = \theta - \beta, \quad (17)$$

and due to the central gear adjustment the new blade angle is

$$\alpha' = \alpha - \frac{\beta}{2} = \frac{\theta'}{2}. \quad (18)$$



(c) Cross Section

**Figure 9:** (a) An isometric view of the turbine solid model. (b) A top view demonstrates the 1:2 gear ratio between the central and satellite gears. (c) The three main assemblies — the central shaft (dark green), rotor (tan), and base (red) — are shown in cross-section.

Because the new blade angle,  $\alpha'$ , is still half the new rotor angle,  $\theta'$ , with respect to the new wind direction, the kinematic constraint is maintained.

Control of the central shaft for adjusting the blade angle can be passive or active. In a passive system, the central shaft could be directly driven by a wind vane. In an active system, a sensor would detect a change in wind direction and a control system would drive a motor to adjust the central shaft orientation. The passive system provides simplicity, while the active system could protect against the central shaft being back driven by the geared system (through the introduction of a worm gear or otherwise). In the author's prototype, a manual adjustment system sufficed, since a fan was the only tested wind source. The prototype has the capability to be upgraded to an actively controlled system.

## 5.4 Blade Design

Because each blade makes only one half of a rotation per full revolution of the rotor, there exists an additional constraint that blades need to be symmetric about their axis under 180-degree rotation. For a rigid blade, this effectively eliminates the option of a "scooped" blade design found on most Savonius turbines. Blades can be aerodynamically formed to minimize form drag during upwind travel, as long as they maintain the required rotational symmetry. For the author's prototype, flat, reinforced, foam blades were used due to their ease of construction.

Alternatively, blades could employ a fabric that acts as a sail, creating a shallow bucket during downwind travel and falling slack during a portion of the upwind travel (and generating no power during this interval). Advantages of this blade type would include a reduced blade weight and a potentially larger downwind drag coefficient. If pursuing this design, care would have to be taken to not suffer the same pitfalls as slatted blade designs discussed in Section 2.1, namely, loss of efficiency due to centrifugal forces on under-constrained blade elements.

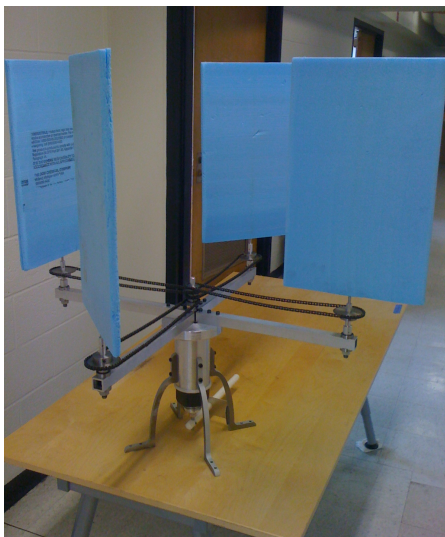
The prototype was designed so that blades can be switched out easily for future testing of different designs for blade optimization (see Section 6.1). The author was only able to construct one set of blades during the course of this project, and was therefore unable to test different blade designs.

## 5.5 Testing

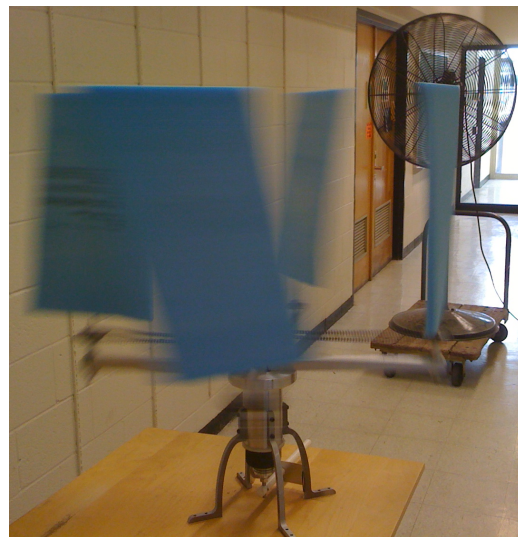
Initial (and hardly comprehensive) testing was performed by placing the prototype turbine downwind of a large fan in a hallway (Fig. 10). The turbine had a start-up wind speed of below  $1.5 \frac{\text{m}}{\text{s}}$ . At an approximate wind speed of  $4 \frac{\text{m}}{\text{s}}$ , and with a rotor position of  $\theta = 0$ , the rotor provided a static torque of approximately 0.8 Nm. With no load, the turbine reached a rotational rate of  $\omega = 70 \text{ rpm}$ .

No machinery for power generation was set up, but interpolating from static torque and no-load speed gives a theoretical power of about 2.9 W, or an efficiency of  $C_P = 0.15$ , before any losses due to power conversion (this is about half of the theoretical efficiency of 0.29, calculated as in Equation 16). While these measurements are very approximate (accurate to at best 30 percent), they indicate the feasibility of achieving high performance with this style turbine. More extensive testing remains to be performed to refine these measurements, and design optimization performed to improve efficiency.

During testing, at 70 rpm the turbine experienced no noticeable wobbling, but the blades leaned backwards significantly during transverse and downwind travel due to drag forces. A combination of stiffer blades and a constraint on the tops of the blades is likely required to remedy this issue.



(a) Stationary prototype turbine



(b) Turbine during testing

**Figure 10:** Prototype turbine, stationary and during testing. In a wind speed of  $4 \frac{\text{m}}{\text{s}}$ , the static torque was about 0.8 Nm and the no-load speed 70 rpm. At this speed, drag forces on the blades caused them to lean backwards significantly.



## 6 Conclusions

The technical analysis of Section 4 demonstrated that this type of turbine is capable of higher efficiencies (Equation 16), slightly higher optimal tip speed ratios (Equation 14), and high static torque (Equation 9) than a typical Savonius Turbine. These increases in performance come at an increase in mechanical complexity, as discussed in Section 5. These tradeoffs, therefore, need to be weighed, and it is likely that this style turbine is most applicable for small scale power generation or mechanical work production, where a small turbine footprint (high efficiency) is required.

Initial testing demonstrated that achieving an efficiency relatively close to the theoretical target presented in Section 4.3 is plausible, and extensive testing should be performed on this prototype to verify the preliminary results presented in Section 5.5. To achieve efficiencies closer to the theoretical values, there remains much optimization to be performed on this prototype, discussed in the next section.

### 6.1 Optimization

There is plenty of room for improvement through future optimization of this design. The size and weight of the prototype rotor assembly were largely driven by economical bearing selection, and so a second generation prototype could significantly reduce rotor inertia and bearing friction. Stiffening and constraining the tops of the turbine blades is also expected to improve efficiency significantly.

Blade style, shape, and dimensions should also undergo extensive testing and optimization. Different blade concepts (e.g. rigid or sail-like, as discussed in Section 5.4) can be considered, and the parameters for each design should be optimized (blade width vs. rotor radius, blade height, etc.).

## References

- [1] Caplan, N. and Gardner, T.N. “A Fluid Dynamic Investigation of the Big Blade and Macon oar Blade Designs in Rowing Propulsion.” *Journal of Sports Sciences*. 25, 6 (2007), pp. 643-650.
- [2] Dieudonne, P. *EolProcess.com*. <<http://www.eolprocess.com>> (accessed April 22, 2010).
- [3] Hoerner, S.F. and Borst, H. *Fluid-Dynamic Lift: Practical Information on Aerodynamic and Hydrodynamic Lift*. Published by Liselotte A. Hoerner, 1985.
- [4] Hwang, I.S. et. al. “Efficiency Improvement of a New Vertical Axis Wind Turbine by Individual Active Control of Blade Motion.” *Proceedings of SPIE*. 6173-11 (2006), <<http://dx.doi.org/10.1117/12.658935>>.
- [5] Jiangsu Wynch Corp., Ltd. “Vertical Axis Variable Pitch Wind-Power Turbine” <<http://wynchn.en.made-in-china.com/product/EbUmIRyCXIVN/China-Vertical-Axis-Variable-Pitch-Wind-Power-Turbine-FDC-HV-Series-.html>> and “Vertical Axis Wind Turbine (VAWT)” <<http://www.youtube.com/watch?v=IE6yDTVR35c>> (accessed April 25, 2010)
- [6] Modi, V.J. and Fernando, M.S.U.K. “On the Performance of the Savonius Wind Turbine.” *Journal of Solar Energy Engineering* 111 (1989), pp. 71-81, <<http://dx.doi.org/10.1115/1.3268289>>.
- [7] Paraschivoiu, I. *Wind Turbine Design: With Emphasis on Darrieus Concept*. Montreal: Polytechnic International Press, 2002.
- [8] Reupke, P. and Probert, S.D. “Slatted-Blade Savonius Wind-Rotors.” *Applied Energy*. 40, 1 (1991), pp. 65-75, <[http://dx.doi.org/10.1016/0306-2619\(91\)90051-X](http://dx.doi.org/10.1016/0306-2619(91)90051-X)>.
- [9] M. Simonds and A. Bodek “Performance Test of a Savonius Rotor.” *Technical report No. T10*. Brace Research Institute, McGill University, Quebec, 1964.
- [10] Tabassum, S.A. and Probert, S.D. “Vertical-Axis Wind Turbine: A Modified Design.” *Applied Energy*. 28, 1 (1987), pp. 59-67, <[http://dx.doi.org/10.1016/0306-2619\(87\)90041-9](http://dx.doi.org/10.1016/0306-2619(87)90041-9)>.